Polymer 124 (2017) 219–225

Contents lists available at ScienceDirect

Polymer

journal homepage: www.elsevier.com/locate/polymer

Atomistic insight into the role of amine groups in thermoresponsive poly(2-dialkylaminoethyl methacrylate)s

Sa Hoon Min [a], Sang Kyu Kwak [b], Byeong-Su Kim [a, c, *]

[a] Department of Energy Engineering, School of Energy and Chemical Engineering, Ulsan National Institute of Science and Technology (UNIST), 50 UNIST-gil, Ulsan 44919, Republic of Korea
[b] Department of Chemical Engineering, School of Energy and Chemical Engineering, Ulsan National Institute of Science and Technology (UNIST), 50 UNIST-gil, Ulsan 44919, Republic of Korea
[c] Department of Chemistry, School of Natural Science, Ulsan National Institute of Science and Technology (UNIST), 50 UNIST-gil, Ulsan 44919, Republic of Korea

ARTICLE INFO

Article history:
Received 15 April 2017
Received in revised form
22 July 2017
Accepted 28 July 2017
Available online 28 July 2017

Keywords:
Thermoresponsive polymer
LCST
MD simulation
Amine group

ABSTRACT

The role of amine groups in the phase separation of thermoresponsive poly(2-dialkylaminoethyl methacrylate)s with dimethyl-, diethyl-, and diisopropylaminoethyl substituents has been studied by atomistic molecular dynamics simulations. The polymer chains present a more compact conformation at higher temperatures, losing contact with the water molecules. In the vicinity of the amine groups, the exclusion of water molecules increases with the increasing hydrophobicity of the amine moieties above the lower critical solution temperature. In particular, the potential of mean force results suggest that the formation of hydrogen bonding between the amine groups and water molecules involves more entropic contributions at higher temperatures in the cases of the diethylaminoethyl and diisopropylaminoethyl groups. These results provide insight for the rational design of side chains of thermoresponsive polymers for smart materials and devices.

1. Introduction

It is well-known that thermoresponsive polymers show conformational transitions in solution around their lower critical solution temperature (LCST), resulting in poor solubility of the polymer chains above that temperature [1,2]. Such changes in solubility have opened up a new horizon for smart materials and devices that respond to changes in the external temperature [3–7]. Over the last decade, molecular dynamics (MD) simulations have provided atomistic information on the conformational transitions, polymer–solvent interactions, and solvent microstructure in thermoresponsive polymer solutions.

Significant research efforts have focused on the LCST behavior of poly(*N*-isopropylacrylamide) (PNIPAM), the most representative thermoresponsive polymer, with single chain systems [8–10], multi-chain systems [11], artificial nanostructures [12,13], drug-delivery applications [14], urea-induced collapse [15,16], co-solvents [17,18], tacticity control [19,20], and copolymerization [21,22] by MD simulation. Most commonly, hydrogen bonding (H-bonding) between the PNIPAM chains and water molecules are weakened, whereas the hydrophobic interactions of isopropyl groups are strengthened in globular conformations of PNIPAM. Such MD calculations have also been extended to a wide range of LCST polymers and polypeptides. As another example of thermoresponsive polymers, the conformational transition of poly(ethylene oxide) (PEO) has been calculated by the Yethiraj group, suggesting that the LCST behavior of PEO in ionic liquids is mainly due to the entropic penalty of the H-bonding between PEO and cations [23–25]. In addition, the Yingling and the Hall group have both demonstrated the LCST behavior of elastin-like polypeptides in aqueous solution and the chain-length dependence on their LCST behavior by atomistic MD simulations [26,27]. Compared to the recent progress on the simulation of LCST behavior, little attention has been paid to the MD simulation of poly(2-dimethylaminoethyl methacrylate), which is responsive to both thermal and pH changes [28].

Fine tuning the temperature- and pH-windows of stimulus-responsive polymers is essential to prepare smart materials and

* Corresponding author. Department of Chemistry, School of Natural Science, Ulsan National Institute of Science and Technology (UNIST), 50 UNIST-gil, Ulsan 44919, Republic of Korea.
E-mail address: bskim19@unist.ac.kr (B.-S. Kim).

http://dx.doi.org/10.1016/j.polymer.2017.07.073
0032-3861/

devices designed to operate under particular external stimuli in nano- and biotechnologies. Typically, the LCST behavior of thermoresponsive polymers is controlled by copolymerization with other monomers [29–32] or small molecules such as ionic liquids [33]. The side chains of thermoresponsive polymers can also be designed to modulate the hydrophilicity, hydrophobicity, or hydrogen bonding ability. Recently, we have reported that the cloud point of PEO-based functional polymers can be widely tuned through their pendant amine groups in terms of their types and hydrophobicity [34]. In parallel, the Plamper group has also demonstrated that the pH and temperature of which the phase separation occur in poly(2-dialkylaminoethyl methacrylate)s are lowered by increasing the hydrophobicity of the dialkylaminoethyl substituents [35]. In particular, by means of fluorescence spectroscopy, they found that the phase separation of poly(2-dimethylaminoethyl methacrylate) is mainly due to backbone/carbonyl interactions, while the phase separation of poly(2-diethylaminoethyl methacrylate) and poly(2-diisopropylaminoethyl methacrylate) is originated from the less polar dialkylaminoethyl groups. Likewise, the type and hydrophobicity of amine moieties in the side chain influence the phase separation of LCST polymers, but theoretical and fundamental understanding of such substituent effects remains to be developed.

In this study, we have carried out MD simulations of the conformational transitions of a series of poly(2- dialkylaminoethyl methacrylate)s as model polymers for investigating the effect of different amine groups on the LCST behavior. Three poly(2-dialkylaminoethyl methacrylate)s with dimethyl-, diethyl-, and diisopropylaminoethyl substituents were evaluated at two different temperature regimes (below and above the LCST). Since our previous study revealed the exclusion of water molecules in the vicinity of carbonyl groups in the phase separation of poly(2-dimethylaminoethyl methacrylate) [36], we here focused on the role of the carbonyl and amine groups in the phase separation of the poly(2-dialkylaminoethyl methacrylate) series. The structural properties of the specific functional groups and water molecules were investigated. In particular, the hydrogen bonding between the amine groups and water molecules was monitored with the potential of mean force (PMF) calculations.

2. Method

2.1. Polymer modeling

The OPLS-AA force field [37] was applied to single chains of poly(2-dialkylaminoethyl methacrylate)s. Atomistic models with the OPLS-AA force field have been reported to successfully reproduce the LCST behavior of PNIPAM [13,20,22]. We modeled syndiotactic polymers with 30 monomer units, owing to the distinct change in the conformational transition [9]. Poly(2-dimethylaminoethyl methacrylate), poly(2-diethylaminoethyl methacrylate), and poly(2-diisopropylaminoethyl methacrylate) are denoted as PDM, PDE, and PDiP, respectively, as shown in Fig. 1. The fully deprotonated states were only considered in order to compare the roles of the carbonyl and deprotonated dialkylaminoethyl groups in the conformational transitions of the polymer. The TIP4P/2005 model [38] was used for explicit water molecules, because the water model is not only one of the best description of water molecules but it has also been used for PNIPAM solution with the OPLS-AA force field [20,22].

2.2. Simulation details

All of the MD simulation were carried out with GROMACS 5.1.2 package [39]. The polymer topologies were generated by MKTOP script [40] for GROMACS-compatible format. The initial polymer conformation with a fully extended chain was relaxed by a short NVT MD simulation without water molecules. Then, each polymer chain was solvated with 12,000 water molecules in a cubic periodic simulation box of side length 7.2 nm. After an energy minimization of the initial system, the equilibration was performed by a short 100-ps NVT ensemble and 500-ps NPT ensemble with a position restraint potential to the polymer chain. Finally, long NPT MD simulations of 300 ns were calculated at two different temperatures, 290 and 330 K. The target temperature was maintained by using a V-rescale thermostat [41] with a coupling constant of 0.1 ps. A Parrinello–Rahman barostat [42] with a coupling constant of 2.0 ps was used to keep the pressure constant at 1.0 bar. For the short-range nonbonded interactions, the cutoff distance was set to 1.0 nm. For considering the long-range electrostatic interactions, the particle mesh Ewald (PME) method [43,44] was employed. All the bond lengths with hydrogen atoms were constrained with the LINCS algorithm [45]. Thus, a time step of 2 fs was applied.

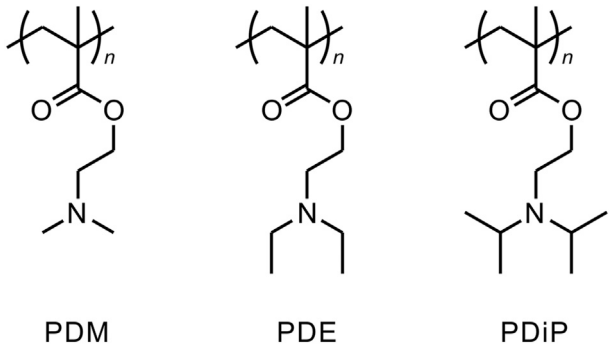

Fig. 1. Molecular structures of poly(2-dimethylaminoethyl methacrylate) (PDM), poly(2-diethylaminoethyl methacrylate) (PDE), and poly(2-diisopropylaminoethyl methacrylate) (PDiP).

The potential of mean force (PMF) was calculated by the umbrella sampling and the weighted histogram analysis method (WHAM) [46]. Each monomer unit was solvated with 3000 explicit water molecules. The distance between the nitrogen atom in the amine group of the monomer and the oxygen atom in a water molecule was restrained by a harmonic potential. Each NPT MD simulation of 10 ns was performed at 25 different distances with 0.05 nm spacing. VMD package [47] was used for the visualization of polymer chains.

3. Results and discussion

Due to the absence of the torsional parameters of the O–C–C–N dihedral in the OPLS-AA force field, we calculated and compared the rotational energy of the torsion angle from *ab initio* [48] and OPLS-AA force field with a 2-dimethylaminoethyl acetate, which is the simplest monomer structure for O–C–C–N dihedral. The molecular structure was scanned with a step size of 15°, based on the O–C–C–N dihedral angle. Fig. 2 shows the overestimated energy barrier of the original OPLS-AA force field (by up to 2 kcal/mol) compared with the *ab initio* calculation at MP2/aug-cc-pVTZ//MP2/cc-pVDZ level. By adding an additional torsional parameter, the energy profile from the fitted OPLS-AA force field was in good agreement with that from the *ab initio* calculation.

Long NPT (*i.e.*, isothermal and isobaric ensemble) MD simulations of 300 ns were performed for single chains of PDM, PDE, and PDiP in water with the fitted torsion parameter at two different temperatures, 290 and 330 K, based on the known LCST of PDM (~40 °C) [49]. Structural analysis was carried out on the

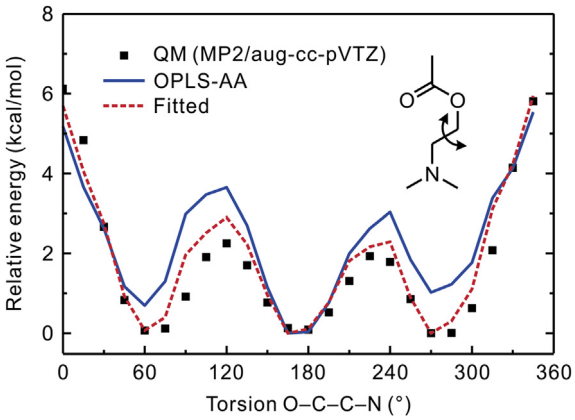

Fig. 2. Rotational energy scan of the O–C–C–N torsion angle with a 2-dimethylaminoethyl acetate molecule at the MP2/aug-cc-pVTZ level (black square), OPLS-AA (blue line), and OPLS-AA with the fitted parameters (red dashed line). (For interpretation of the references to colour in this figure legend, the reader is referred to the web version of this article.)

last 100 ns trajectories. Fig. 3 displays the contour plots of the radius of gyration (R_g) versus the solvent accessible surface area (SASA) for PDM, PDE, and PDiP single chains. These two parameters are representing the dimensional properties of polymer chains in solution, which are calculated by the mass-weighted root-mean-square of the average distance of each atom from the center-of-mass position and the double cubic lattice method [50], respectively.

In all cases, both R_g and SASA decreased with the increasing temperature, indicating that the polymer chains display more compact conformations at higher temperatures. In particular, the single chain of PDM showed a distinct conformation transition between 290 and 330 K with the largest reduction in the most populated R_g ($\Delta = -0.17$ nm) and SASA ($\Delta = -4.8$ nm^2) (Fig. 3a). Interestingly, this conformation transition of PDM is consistent with our previous observation with the PCFF force field [36]. A partially linear conformation was also observed at 290 K, and a compact globular conformation was observed at 330 K. In the cases of PDE and PDiP, however, the polymer chains showed a more compact conformation even at 290 K in comparison with the PDM chain, due to the more hydrophobic alkyl substituents of PDE and PDiP (Fig. 3b and c). It must be noted that the low solubility of deprotonated PDE and PDiP in water has also been observed experimentally, exhibiting thermoresponsive behavior only within a narrow pH range [35]. The fully deprotonated models in this study were not intended to reproduce the exact LCSTs, but to provide insight into the role of certain functional groups in LCST behavior. Despite the already compact conformation at 290 K, it can be seen that the PDE and PDiP conformations at 330 K are even more

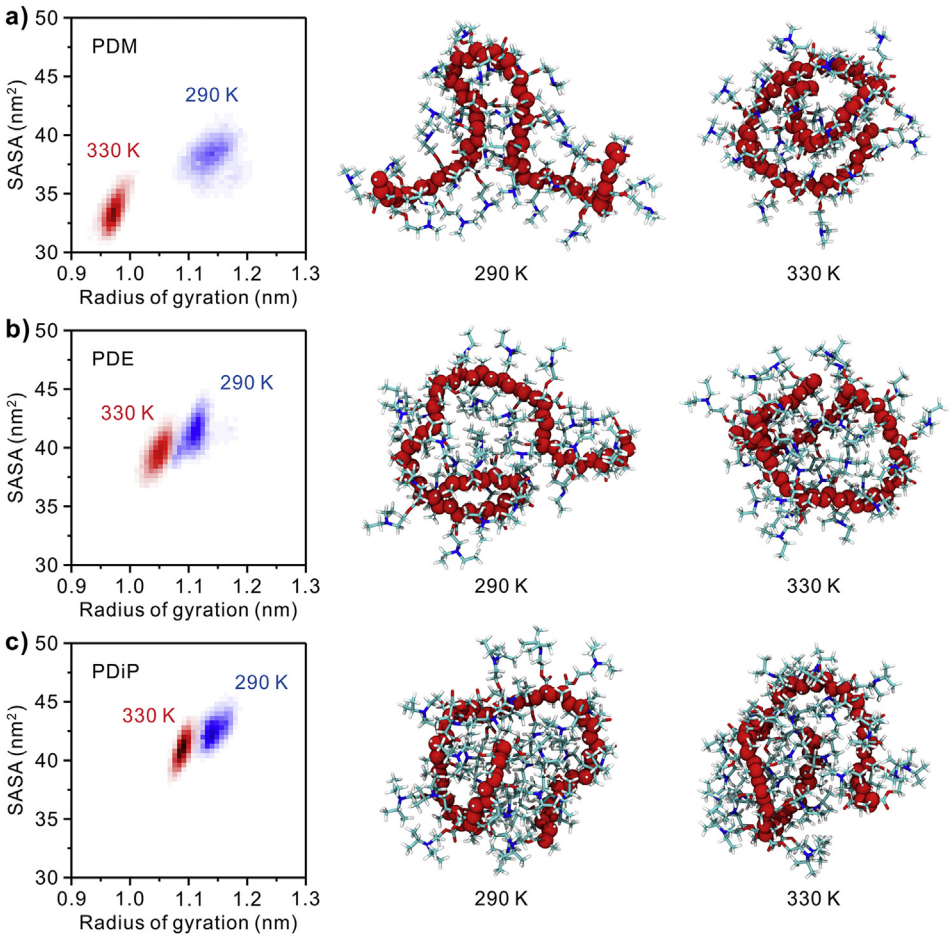

Fig. 3. Contour plots of the radius of gyration (R_g) and solvent accessible surface area (SASA) of (a) PDM, (b) PDE, and (c) PDiP single chains from the last 100 ns of production runs at 290 and 330 K. The most populated conformations at each temperature are shown on the right. For clarity, the backbone carbon atoms are represented by large red beads, and water molecules are not shown. (For interpretation of the references to colour in this figure legend, the reader is referred to the web version of this article.)

condensed, although by a smaller difference of the most populated SASAs ($\Delta = -1.6$ and -0.8 nm^2, respectively), as summarized in Table 1.

The conformation analysis through the R_g and SASA parameters revealed that single chains of poly(2-dialkylaminoethyl methacrylate) lost contact with water molecules at high temperature. To clarify the structural features between the polymer and water molecules, the radial distribution functions (RDFs) of the carbonyl oxygen (Oc) and amine nitrogen (N) in poly(2-dialkylaminoethyl methacrylate) relative to the water oxygen (Ow) were calculated from the last 100 ns of the simulations (Fig. 4a and b).

Fig. 4c shows the Oc–Ow RDFs of PDM, PDE, and PDiP at 290 K and 330 K. In all cases, the same peak at 0.28 nm and the same first hydration shell at 0.33 nm were observed. The intensity of the first peak at 0.28 nm in the Oc–Ow RDF of PDM decreased with the increasing temperature, suggesting that the water molecules in the vicinity of the carbonyl group of PDM were expelled in the globular conformation. Such expulsion of water molecules near the carbonyl groups of PDM was also observed in concert with our previous work [36]. In contrast, the intensity of the peak of the Oc–Ow RDF of PDE and PDiP decreased slightly for the first hydration shell at 330 K, resulting from the compact conformation below the LCST.

Fig. 4d displays the RDF of the N atom in the amine group to the Ow atom in water. The second hydration shell (*i.e.*, the second minimum of the N–Ow RDFs) increased from 0.61 nm up to 0.70 nm, and the shoulder peak at 0.58 nm became dominant with the increasing hydrophobicity of the alkyl substituents. In contrast to the previous work [36], a strong first hydration shell was observed with a peak at 0.29 nm, indicating that the amine groups in the polymer can readily establish H-bonds with water molecules. In all cases, the intensity of the peaks corresponding to the first and second hydration shells decreased with the increasing temperature.

To quantitatively assess the contact of water molecules at the functional groups of the polymer chains, we have concentrated on the average number of water molecules per functional group unit in the first hydration shell (N_W) of the Oc and N atoms and the average number of H-bonds per functional group unit (N_{HW}) between the functional groups and water molecules. The N_W and N_{HW} were calculated by integrating the RDFs in Fig. 4 from zero to the first hydration shell radius (~3.5 Å) and by using the geometric criteria of the donor, acceptor, and hydrogen atoms, respectively. Specifically, distances between donor and acceptor atoms below 3.5 Å and angles between hydrogen–donor and donor–acceptor vectors smaller than 30° were considered to form an effective H-bonding.

Fig. 5 shows the N_W values for the Oc and N atoms and the N_{HW} values for the Oc–Ow and N–Ow atoms at two different temperatures. In the case of the carbonyl groups, N_W was higher than N_{HW}, meaning that there were water molecules in the first hydration shell not participating in H-bonding. On the other hand, the N_W and N_{HW} values for the amine groups were almost identical, indicating that most of water molecules in the first hydration shell of the N atoms participate in H-bonding with the amine groups, as a result of the steric hindrance induced by the dialkyl groups.

As shown in Fig. 5a, the N_{HW} between the carbonyl groups and water molecules for PDM was significantly reduced by 20.3% at 330 K. In contrast, a moderate reduction of 7.1% was observed for the N_{HW} between the amine groups of PDM and water molecules, indicating that the amine groups of PDM are well in contact with water molecules even in the globule state. These results are consistent with the results of a previous experimental study, in which the phase separation of PDM was found to be mainly due to backbone/carbonyl interactions [35]. Upon increasing the hydrophobicity of the dialkyl group, the N_{HW} between the amine groups and water molecules decreased considerably.

Interestingly, at 330 K, it can be seen that the decreasing trend for the N_{HW} between the amine groups and water molecules in PDE and PDiP was further enhanced by 13.2% and 42.6%, respectively (Fig. 5b and c). On the other hand, the N_{HW} between the carbonyl groups and water molecules decreased very slightly or even increased for the PDE and PDiP chains upon increasing the temperature. This hydration state of the deprotonated amine group is distinct from that of the protonated amine group. The protonation enabled the PDiP chain, the most hydrophobic case, to be water-soluble, but the hydration state of the amine group was not significantly sensitive to the temperature, as shown in Figs. S1 and S2, respectively.

Taking into account the microstructure between water molecules and the functional groups in poly(2-dialkylaminoethyl methacrylate)s, it suggests that the amine groups in PDE and PDiP play an important role in the phase separation, with a conformational transition from globule-like structures to more compact conformations. In addition, these structural features support the recently reported observation on the phase separation of PDE and PDiP solutions, which was mainly attributed to the low polarity of the dialkylaminoethyl groups, affording drastic changes in the hydrophobic environment around the cloud point [35].

Fig. 6 shows the PMF calculations along the distance between the N atom in the monomer units of PDM, PDE, and PDiP and an Ow atom at 290 and 330 K. The first minimum at ~2.8 Å and the first maximum at ~3.5 Å in the PMF plots are correlated with the H-bonding between the amine groups and water molecules, and the first hydration shell of the N atoms, respectively. The first minimum of the PMF plots represents entropic cost of the formation of such H-bonding [24]. In the case of the monomer unit of PDM, the PMF

Table 1
Summary of structural properties of PDM, PDE, and PDiP at 290 and 330 K.[a]

Polymer	Temperature (K)	R_g (nm)[b]	SASA (nm^2)[c]	N_W[d]		N_{HW}[e]	
				Carbonyl group	Amine group	Carbonyl group	Amine group
PDM	290	1.14	38.4	1.31	0.87	0.79	0.84
	330	0.97	33.6	1.04 (20.6%)	0.82 (5.7%)	0.63 (20.3%)	0.78 (7.1%)
PDE	290	1.11	41.2	1.14	0.77	0.73	0.76
	330	1.05	39.6	1.11 (2.6%)	0.68 (11.7%)	0.67 (8.2%)	0.66 (13.2%)
PDiP	290	1.14	42.0	1.18	0.48	0.77	0.47
	330	1.11	41.2	1.27 (−7.6%)	0.28 (41.7%)	0.80 (−3.9%)	0.27 (42.6%)

[a] The structural properties were calculated from the last 100 ns of production runs at 290 and 330 K.
[b] The most populated radius gyration, R_g.
[c] The most populated solvent accessible surface area, SASA.
[d] Average number of water molecules per each functional group unit in the first hydration shell and the decreasing rate at 330 K (in parentheses).
[e] Average number of hydrogen bonds per each functional group unit to water molecules and the decreasing rate at 330 K (in parentheses).

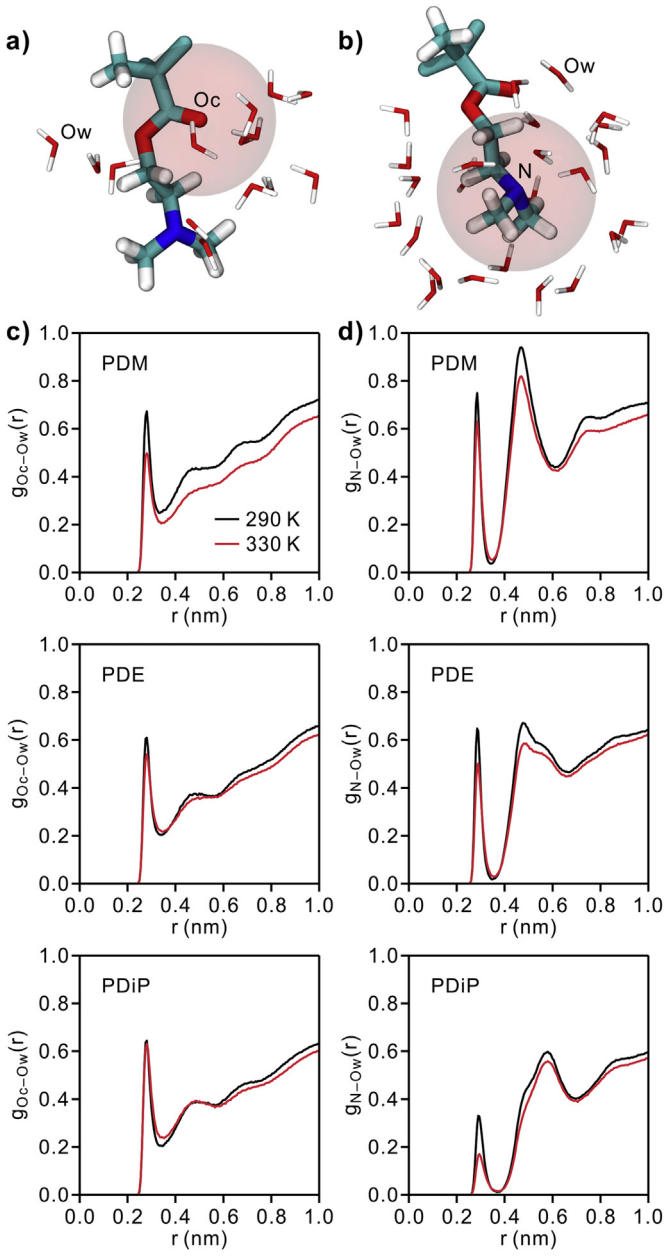

Fig. 4. Snapshots of a PDM monomer unit with water molecules in the second hydration shell of (a) the carbonyl oxygen (Oc) and (b) the amine nitrogen (N) at 290 K. The transparent red sphere represents the first hydration shell of each atom. Radial distribution functions (RDFs) of the (c) Oc and (d) N in PDM, PDE, and PDiP relative to water oxygen (Ow) at 290 and 330 K. (For interpretation of the references to colour in this figure legend, the reader is referred to the web version of this article.)

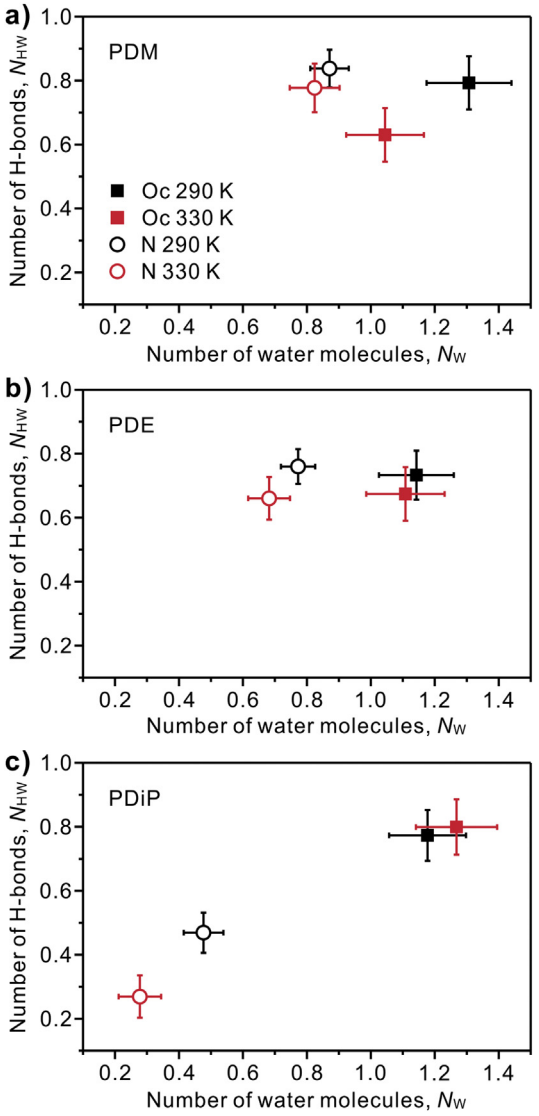

Fig. 5. Average number of water molecules per functional group unit in the first hydration shell (N_W) of the Oc and N atoms versus the average number of hydrogen bonds per functional group unit (N_{HW}) between the functional groups and water molecules for single chains of (a) PDM, (b) PDE, and (c) PDiP at 290 and 330 K.

curves at 290 and 330 K are almost identical, and the difference between the PMF at the first minimum is only 0.06 kcal/mol, as shown in Fig. 6a. However, the first minimum in the PMF of the PDE and PDiP monomer units increases with the temperature (Fig. 6b and c), with differences of 0.13 and 0.44 kcal/mol, respectively. It is obvious that the H-bonding between the diethylaminoethyl group and water molecules and between the diisopropylaminoethyl groups and water molecules involves more entropic cost at higher temperatures. Thus, it can be concluded that, with the increasing temperature, the H-bonds between water and the PDE and PDiP amine groups present a more restricted conformation than those in PDM due to steric hindrance, resulting in the exclusion of water molecules in the vicinity of the diethylaminoethyl and diisopropylaminoethyl groups.

4. Conclusions

In conclusion, we have successfully performed atomistic MD simulations to compare the LCST behavior of single chains of poly(2-dialkylaminoethyl methacrylate)s with dimethyl, diethyl, and diisopropyl substituents. Poly(2-dialkylaminoethyl methacrylate)s were found to lose contact with water molecules at temperatures above the LCST. In particular, the exclusion of water molecules by the dialkylaminoethyl groups increased with the increasing hydrophobicity of the amine moieties, indicating the importance of the amine groups in the LCST behavior of polymers. Furthermore, the H-bonding between the amine groups and water molecules was found to involve more entropic contributions at higher temperatures in the cases of the diethylaminoethyl and diisopropylaminoethyl groups. These results provide fundamental

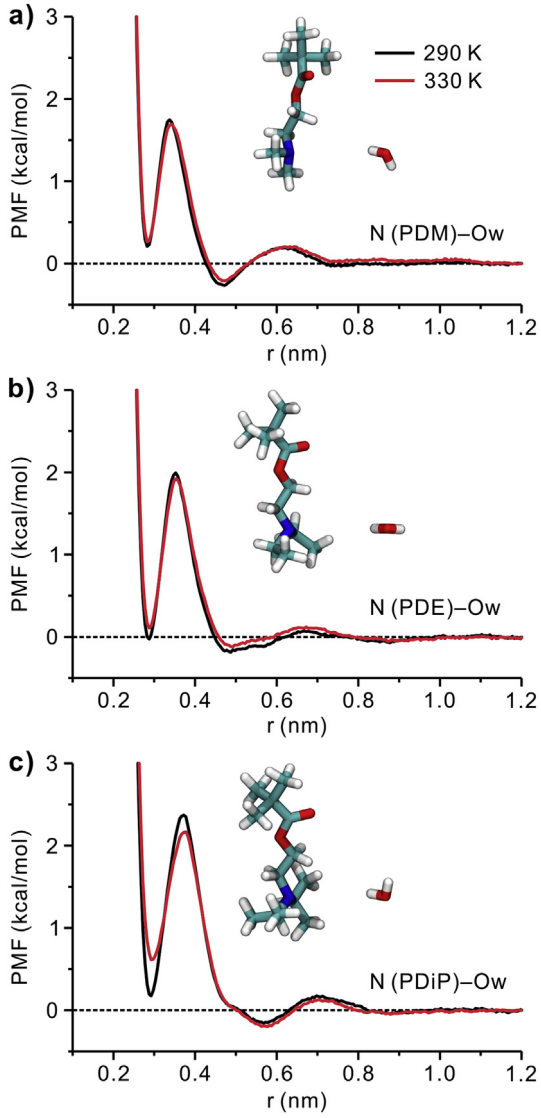

Fig. 6. Potential of mean force (PMF) along the distance between the N atom in (a) PDM, (b) PDE, and (c) PDiP monomer units and the Ow atom at 290 and 330 K.

insight into the LCST behavior of poly(2-dialkylaminoethyl methacrylate)s with different hydrophobic amine moieties. It is also expected that such a theoretical model will aid the rational design of side chains for thermoresponsive polymers.

Acknowledgment

This work was supported by the 2017 Research Fund (1.170084.01) of UNIST (Ulsan National Institute of Science and Technology). Computational resources are from UNIST-HPC and KISTI-PLSI.

Appendix A. Supplementary data

Supplementary data related to this article can be found at http://dx.doi.org/10.1016/j.polymer.2017.07.073.

References

[1] Y. Katsumoto, T. Tanaka, H. Sato, Y. Ozaki, Conformational change of poly(N-isopropylacrylamide) during the Coil–Globule transition investigated by attenuated total reflection/infrared spectroscopy and density functional theory calculation, J. Phys. Chem. A 106 (2002) 3429–3435.
[2] S. Rimmer, I. Soutar, L. Swanson, Switching the conformational behaviour of poly(N-isopropyl acrylamide), Polym. Int. 58 (2009) 273–278.
[3] M.A.C. Stuart, W.T.S. Huck, J. Genzer, M. Müller, C. Ober, M. Stamm, G.B. Sukhorukov, I. Szleifer, V.V. Tsukruk, M. Urban, F. Winnik, S. Zauscher, I. Luzinov, S. Minko, Emerging applications of stimuli-responsive polymer materials, Nat. Mater 9 (2010) 101–113.
[4] N. Badi, Non-linear PEG-based thermoresponsive polymer systems, Prog. Polym. Sci. 66 (2017) 54–79.
[5] R. Liu, M. Fraylich, B.R. Saunders, Thermoresponsive copolymers: from fundamental studies to applications, Colloid Polym. Sci. 287 (2009) 627–643.
[6] N. Rapoport, Physical stimuli-responsive polymeric micelles for anti-cancer drug delivery, Prog. Polym. Sci. 32 (2007) 962–990.
[7] F. Liu, M.W. Urban, Recent advances and challenges in designing stimuli-responsive polymers, Prog. Polym. Sci. 35 (2010) 3–23.
[8] S.A. Deshmukh, S.K.R.S. Sankaranarayanan, K. Suthar, D.C. Mancini, Role of solvation dynamics and local ordering of water in inducing conformational transitions in poly(N-isopropylacrylamide) oligomers through the LCST, J. Phys. Chem. B 116 (2012) 2651–2663.
[9] A.K. Tucker, M.J. Stevens, Study of the polymer length dependence of the single chain transition temperature in syndiotactic poly(N-isopropylacrylamide) oligomers in water, Macromolecules 45 (2012) 6697–6703.
[10] H. Du, S.R. Wickramasinghe, X. Qian, Specificity in cationic interaction with poly(N-isopropylacrylamide), J. Phys. Chem. B 117 (2013) 5090–5101.
[11] M. Alaghemandi, E. Spohr, Molecular dynamics investigation of the thermo-responsive polymer poly(N-isopropylacrylamide), Macromol. Theory Simul. 21 (2012) 106–112.
[12] M. Alaghemandi, E. Spohr, A molecular dynamics study of poly(N-isopropylacrylamide) endgrafted on a model cylindrical pore surface, RSC Adv. 3 (2013) 3638–3647.
[13] L. Lorbeer, M. Alaghemandi, E. Spohr, Molecular dynamics studies of poly(N-isopropylacrylamide) endgrafted on the surfaces of model slab pores, J. Mol. Liq. 189 (2014) 57–62.
[14] S. Moghadam, R.G. Larson, Assessing the efficacy of poly(N-isopropylacrylamide) for drug delivery applications using molecular dynamics simulations, Mol. Pharm. 14 (2017) 478–491.
[15] F. Rodríguez-Ropero, N.F.A. van der Vegt, On the urea induced hydrophobic collapse of a water soluble polymer, Phys. Chem. Chem. Phys. 17 (2015) 8491–8498.
[16] S. Micciulla, J. Michalowsky, M.A. Schroer, C. Holm, R. von Klitzing, J. Smiatek, Concentration dependent effects of urea binding to poly(N-isopropylacrylamide) brushes: a combined experimental and numerical study, Phys. Chem. Chem. Phys. 18 (2016) 5324–5335.
[17] J. Walter, J. Sehrt, J. Vrabec, H. Hasse, Molecular dynamics and experimental study of conformation change of poly(N-isopropylacrylamide) hydrogels in mixtures of water and methanol, J. Phys. Chem. B 116 (2012) 5251–5259.
[18] D. Mukherji, M. Wagner, M.D. Watson, S. Winzen, T.E. de Oliveira, C.M. Marques, K. Kremer, Relating side chain organization of PNIPAm with its conformation in aqueous methanol, Soft Matter 12 (2016) 7995–8003.
[19] T.E. de Oliveira, D. Mukherji, K. Kremer, P.A. Netz, Effects of stereochemistry and copolymerization on the LCST of PNIPAm, J. Chem. Phys. 146 (2017) 34904.
[20] E. Chiessi, G. Paradossi, Influence of tacticity on hydrophobicity of poly(N-isopropylacrylamide): a single chain molecular dynamics simulation study, J. Phys. Chem. B 120 (2016) 3765–3776.
[21] R. Singh, S.A. Deshmukh, G. Kamath, S.K.R.S. Sankaranarayanan, G. Balasubramanian, Controlling the aqueous solubility of PNIPAM with hydrophobic molecular units, Comput. Mater. Sci. 126 (2017) 191–203.
[22] L.J. Abbott, A.K. Tucker, M.J. Stevens, Single chain structure of a poly(N-isopropylacrylamide) surfactant in water, J. Phys. Chem. B 119 (2015) 3837–3845.
[23] J.G. McDaniel, E. Choi, C.-Y. Son, J.R. Schmidt, A. Yethiraj, Conformational and dynamic properties of poly(ethylene oxide) in an ionic liquid: development and implementation of a first-principles force field, J. Phys. Chem. B 120 (2016) 231–243.
[24] E. Choi, A. Yethiraj, Entropic mechanism for the lower critical solution temperature of poly(ethylene oxide) in a room temperature ionic liquid, ACS Macro Lett. 4 (2015) 799–803.
[25] J. Mondal, E. Choi, A. Yethiraj, Atomistic simulations of poly(ethylene oxide) in water and an ionic liquid at room temperature, Macromolecules 47 (2014) 438–446.
[26] B. Zhao, N.K. Li, Y.G. Yingling, C.K. Hall, LCST behavior is manifested in a single molecule: elastin-like polypeptide (VPGVG)n, Biomacromolecules 17 (2016) 111–118.
[27] N.K. Li, F.G. Quiroz, C.K. Hall, A. Chilkoti, Y.G. Yingling, Molecular description of the LCST behavior of an elastin-like polypeptide, Biomacromolecules 15 (2014) 3522–3530.
[28] J. Niskanen, C. Wu, M. Ostrowski, G.G. Fuller, S. Hietala, H. Tenhu, Thermoresponsiveness of PDMAEMA. Electrostatic and stereochemical effects, Macromolecules 46 (2013) 2331–2340.
[29] C. Weber, R. Hoogenboom, U.S. Schubert, Temperature responsive biocompatible polymers based on poly(ethylene oxide) and poly(2-oxazoline)s, Prog. Polym. Sci. 37 (2012) 686–714.

[30] M. Glassner, K. Lava, V.R. de la Rosa, R. Hoogenboom, Tuning the LCST of poly(2-cyclopropyl-2-oxazoline) via gradient copolymerization with 2-ethyl-2-oxazoline, J. Polym. Sci. Part A Polym. Chem. 52 (2014) 3118–3122.
[31] S. Reinicke, P. Espeel, M.M. Stamenović, F.E. Du Prez, One-pot double modification of p(NIPAAm): a tool for designing tailor-made multiresponsive polymers, ACS Macro Lett. 2 (2013) 539–543.
[32] S.-H. Jung, H.-I. Lee, Well-defined thermoresponsive copolymers with tunable LCST and UCST in water, Bull. Korean Chem. Soc. 35 (2014) 501–504.
[33] K. Jain, R. Vedarajan, M. Watanabe, M. Ishikiriyama, N. Matsumi, Tunable LCST behavior of poly(N-isopropylacrylamide/ionic liquid) copolymers, Polym. Chem. 6 (2015) 6819–6825.
[34] J. Lee, A.J. McGrath, C.J. Hawker, B.-S. Kim, Ph-tunable thermoresponsive PEO-based functional polymers with pendant amine groups, ACS Macro Lett. 5 (2016) 1391–1396.
[35] T. Thavanesan, C. Herbert, F.A. Plamper, Insight in the phase separation peculiarities of poly(dialkylaminoethyl methacrylate)s, Langmuir 30 (2014) 5609–5619.
[36] S.H. Min, S.K. Kwak, B.-S. Kim, Atomistic simulation for coil-to-globule transition of poly(2-dimethylaminoethyl methacrylate), Soft Matter 11 (2015) 2423–2433.
[37] W.L. Jorgensen, D.S. Maxwell, J. Tirado-Rives, Development and testing of the OPLS all-atom force field on conformational energetics and properties of organic liquids, J. Am. Chem. Soc. 118 (1996) 11225–11236.
[38] J.L.F. Abascal, C. Vega, A general purpose model for the condensed phases of water: TIP4P/2005, J. Chem. Phys. 123 (2005) 234505.
[39] M.J. Abraham, T. Murtola, R. Schulz, S. Páll, J.C. Smith, B. Hess, E. Lindahl, GROMACS: high performance molecular simulations through multi-level parallelism from laptops to supercomputers, SoftwareX 1–2 (2015) 19–25.
[40] A.A.S.T. Ribeiro, B.A.C. Horta, R.B. de Alencastro, MKTOP: a program for automatic construction of molecular topologies, J. Braz. Chem. Soc. 19 (2008) 1433–1435.
[41] G. Bussi, D. Donadio, M. Parrinello, Canonical sampling through velocity rescaling, J. Chem. Phys. 126 (2007) 14101.
[42] M. Parrinello, A. Rahman, Polymorphic transitions in single crystals: a new molecular dynamics method, J. Appl. Phys. 52 (1981) 7182–7190.
[43] T. Darden, D. York, L. Pedersen, Particle mesh Ewald: an N·log(N) method for Ewald sums in large systems, J. Chem. Phys. 98 (1993) 10089–10092.
[44] U. Essmann, L. Perera, M.L. Berkowitz, T. Darden, H. Lee, L.G. Pedersen, A smooth particle mesh Ewald method, J. Chem. Phys. 103 (1995) 8577–8593.
[45] B. Hess, H. Bekker, H.J.C. Berendsen, J.G.E.M. Fraaije, LINCS: a linear constraint solver for molecular simulations, J. Comput. Chem. 18 (1997) 1463–1472.
[46] S. Kumar, J.M. Rosenberg, D. Bouzida, R.H. Swendsen, P.A. Kollman, THE weighted histogram analysis method for free-energy calculations on biomolecules. I. The method, J. Comput. Chem. 13 (1992) 1011–1021.
[47] W. Humphrey, A. Dalke, K. Schulten, VMD: visual molecular dynamics, J. Mol. Graph 14 (1996) 33–38.
[48] M.J. Frisch, G.W. Trucks, H.B. Schlegel, G.E. Scuseria, M.A. Robb, J.R. Cheeseman, G. Scalmani, V. Barone, B. Mennucci, G.A. Petersson, H. Nakatsuji, M. Caricato, X. Li, H.P. Hratchian, A.F. Izmaylov, J. Bloino, G. Zheng, J.L. Sonnenberg, M. Hada, M. Ehara, K. Toyota, R. Fukuda, J. Hasegawa, M. Ishida, T. Nakajima, Y. Honda, O. Kitao, H. Nakai, T. Vreven, J.A. Montgomery Jr., J.E. Peralta, F. Ogliaro, M. Bearpark, J.J. Heyd, E. Brothers, K.N. Kudin, V.N. Staroverov, R. Kobayashi, J. Normand, K. Raghavachari, A. Rendell, J.C. Burant, S.S. Iyengar, J. Tomasi, M. Cossi, N. Rega, N.J. Millam, M. Klene, J.E. Knox, J.B. Cross, V. Bakken, C. Adamo, J. Jaramillo, R. Gomperts, R.E. Stratmann, O. Yazyev, A.J. Austin, R. Cammi, C. Pomelli, J.W. Ochterski, R.L. Martin, K. Morokuma, V.G. Zakrzewski, G.A. Voth, P. Salvador, J.J. Dannenberg, S. Dapprich, A.D. Daniels, O. Farkas, J.B. Foresman, J.V. Ortiz, J. Cioslowski, D.J. Fox, Gaussian 09, Revision C.01, Gaussian Inc, Wallingford CT, 2010.
[49] V. Bütün, S.P. Armes, N.C. Billingham, Synthesis and aqueous solution properties of near-monodisperse tertiary amine methacrylate homopolymers and diblock copolymers, Polymer 42 (2001) 5993–6008.
[50] F. Eisenhaber, P. Lijnzaad, P. Argos, C. Sander, M. Scharf, The double cubic lattice method: efficient approaches to numerical integration of surface area and volume and to dot surface contouring of molecular assemblies, J. Comput. Chem. 16 (1995) 273–284.